Experimental Demonstration of Superimposed Probabilistic 16CAP With the Joint Chaotic Model in a Multi-Core Transmission System

Yu Gu [ID], Feng Tian [ID], Tianze Wu [ID], Jue Wang, Qi Zhang [ID], Qinghua Tian [ID], Yongjun Wang [ID], Rahat Ullah [ID], and Xiangjun Xin [ID]

Abstract—In this paper, we propose a novel carrier-less amplitude/phase modulation with probabilistic shaping based on the Lorenz model and superposition method (LS-PS-CAP). The chaotic model is used to change the probability distribution of the constellation, and superimpose the constellations to obtain LS-PS-16CAP. The proposed scheme can increase modulation flexibility and improve BER performance, and it can also provide security for the transmission system. The transmission of 189.6 Gb/s LS-PS-16CAP data signal over a 2.5 km multi-core fiber (MCF) is experimentally demonstrated. Moreover, the LS-PS-16CAP obtains an average gain of 0.7 dB with the entropy of 3.7bits/symbol compared to the Maxwell-Boltzmann (MB)-PS-16CAP in MCF. The findings suggest that the proposed scheme has a promising future for short-range optical transmission system.

Index Terms—3D constellation, chaotic encryption, carrier-less amplitude, phase modulation, multi-core fiber, and probabilistic shaping.

I. INTRODUCTION

DUE to rapid developments and advancements in technology, the desire for high bandwidth and throughput has been increased by the end-users in optical access systems [1], where cost and complexity are two important factors. Intensity Modulation/Direct Detection (IM/DD) is an optimal selection for next-generation short-distance high-speed optical transmission system due to their simple structure and low cost. Meanwhile, carrier-less amplitude/phase modulation (CAP) has become a widely used modulation scheme in IM/DD systems with the advantages of low complexity and high efficiency [2], [3].

Geometric shaping technology [4]–[6] and probabilistic shaping technology [7] have been extensively studied to improve the performance of the transmission system. Geometric shaping is realized by optimizing the constellation structure so that the constellation diagram is distributed at unequal intervals to expand Euclidean distance and improve the shaping gain. The principle of probabilistic shaping is to optimize the probability distribution of the symbols according to the characteristics of the Gaussian channel to obtain a high shaping gain, which can overcome the nonlinear effect when the power is low [8], [9]. The scheme of three 32QAM constellations with hierarchical levels design was demonstrated in [10], where the experimental results confirm that the system with the square-shaped 8QAM achieves the best BER performance. A novel 3-dimensional probabilistically shaped carrier-less amplitude-phase (3D-PS-CAP) modulation based on constellation design using regular tetrahedron cells was proposed in [11], the results show that at the BER of 1×10^{-3}, the proposed uniform 3D-CAP-16 outperforms the traditional counterparts by 1.1 dB receiver sensitivity gain. A probabilistic allocation scheme based on feedback mechanism was proposed in [12], after optimizing the distribution entropy, the results show that the shaped constellation has better SER performance than the uniformed constellation. A new bit-class PS scheme employing bit weighted distribution matching was proposed in [13], the experiment results show that the proposed scheme can improve 0.407 dB shaping gain and 0.53 dB optical receiver power sensitivity compared with the standard unshaped one. Geometric shaping technology and probabilistic shaping technology can greatly improve shaping gain and receiver power sensitivity compared to traditional uniform modulation scheme.

Scrambling QAM symbols with chaotic models in physically secure optical communications is a hot topic in recent years [14]–[16]. A constellation-shaping chaotic encryption (CSCEn) scheme with a controlled statistical distribution is proposed in [17], and experimental results show that the scheme can improve transmission performance and provide security against attacks. A four-dimensional chaos is proposed to improve the FBMC/OQAM system physical layer security performance with a key space of 10^{90} in [18]. A novel scheme to realize probabilistic shaping and chaotic encryption based on a four-dimensional hyperchaotic Lv system was proposed in [19], 25 km standard single mode fiber (SSMF) transmission system verifies the superiority of the scheme. Traditional encryption schemes use chaotic sequences to scramble the constellation points, making the distribution of constellation points irregular in order to improve the security performance of the system. However, in this paper, probabilistic shaping is directly implemented by using a chaotic model and improves the security performance of the transmission system at the same time.

Yu Gu, Feng Tian, Tianze Wu, Jue Wang, Qi Zhang, Qinghua Tian, Yongjun Wang, and Xiangjun Xin are with the State Key Laboratory of Information Photonics and Optical Communications, Beijing University of Posts and Telecommunications, Beijing 100876, China (e-mail: 2997568046@qq.com; tianfeng@bupt.edu.cn; wutianze@bupt.edu.cn; 985346139@qq.com; zhangqi@bupt.edu.cn; tianqh@bupt.edu.cn; wangyj@bupt.edu.cn; xjxin@bupt.edu.cn).

Rahat Ullah is with the Institute of Optics and Electronics, Nanjing University of Information Science and Technology, Nanjing 210044, China (e-mail: rahat@nuist.edu.cn).
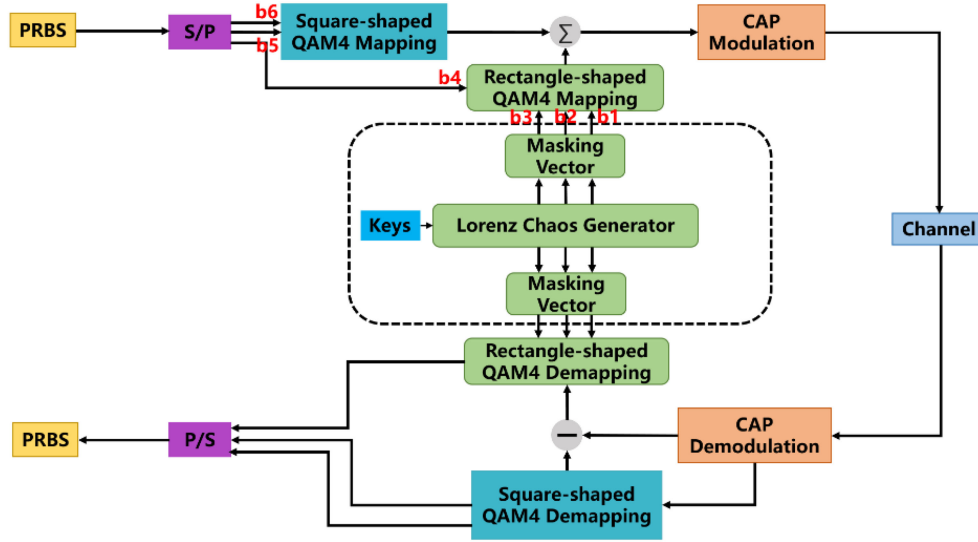
Fig. 1.   Schematic diagram of a new probabilistic shaping based on CAP.
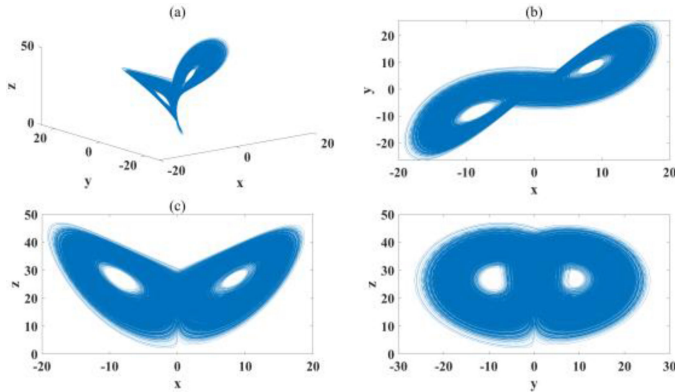

Fig. 2.   The projections of the chaotic attractor of Lorenz chaotic system in the three-dimensional space.

TABLE I
PROBABILITY DISTRIBUTION RULES OF EACH QUADRANT

	TX1/First quadrant	TX1/Second quadrant	TX1/Third quadrant	TX1/Fourth quadrant
TX2/P1	1/16	4/16	8/16	3/16
TX2/P2	4/16	1/16	3/16	8/16
TX2/P3	8/16	3/16	1/16	4/16
TX2/P4	3/16	8/16	4/16	1/16

The capacity of optical communication based on single-mode fiber has been towards the Shannon limit, the high-capacity optical communication system has been the focus of research in recent years. Space division multiplexing (SDM) technology using MCF [20], few-mode fiber (FMF), or MC-FMF is a new direction to increase the transmission capacity [21]. Among them, weakly-coupled MCF transmission is one of the most widely used SDM technologies, which can improve the capacity by increasing the number of cores and effectively reduce inter-core crosstalk by arranging the core spacing. Moreover, it can be widely used in the optical access network for a huge number of users and can decrease the complexity of the system. The main classifications and features of novel space-division multiplexing

(SDM) were outlined in [22]. Similarly, the transmission of 368-WDM-38-core-3-mode × 24.5-GBaud 64 and 256-QAM signals over a range of 13 km, record data rates, and spectral efficiency of 1158.7 b/s/Hz over low DMD 38-core 3-mode was demonstrated in [23]. Space-division multiplexed transmission in the S-band over 55 km few-mode fiber with wavelength channels between 1491.5 nm and 1517.9 nm, demonstrating the feasibility of combining few-mode fibers with S-band transmission [24]. Therefore, SDM technology is seen as an important solution to solve the capacity crisis in optical transmission system.

In this paper, we propose a novel scheme of probabilistic shaping based on the Lorenz model and superposition method (LS-PS-CAP), which can be disassembled into a superposition of two 4QAM structures, where one 4QAM constellation with equal probability distribution and another 4QAM signal with unequal probability distribution are realized using the Lorenz chaotic model. Compared to the traditional ones, the LS-PS-16CAP constellation diagram has lower average energy and high security and can effectively improve the BER performance. To demonstrate the transmission performance of LS-PS-16CAP, we successfully implemented LS-PS-16CAP transmission over a 2.5 km 7-core fiber.

II. PRINCIPLE

The schematic presentation of LS-PS-16CAP is shown in Fig. 1. By using serial to parallel conversion at the transmitter, the random pseudo-random bit sequences are converted into three parallel sequences {b6, b5, b4}. The bit sequences {b6, b5} are used to map square-shaped 4QAM directly. Obtain the following three bits sequences {b3, b2, b1} from the chaotic sequences generated by the Lorenz chaotic model. The bit sequences b4, b3, b2, and b1 are mapped to rectangle-shaped 4QAM. Square-shaped 4QAM and rectangle-shaped 4QAM are superimposed together to obtain the LS-PS-16QAM. Then the signals are convoluted with two mutually orthogonal filters and finally get the LS-PS-16CAP. The opposite operation to the transmitter is performed at the receiver to obtain the original bits.
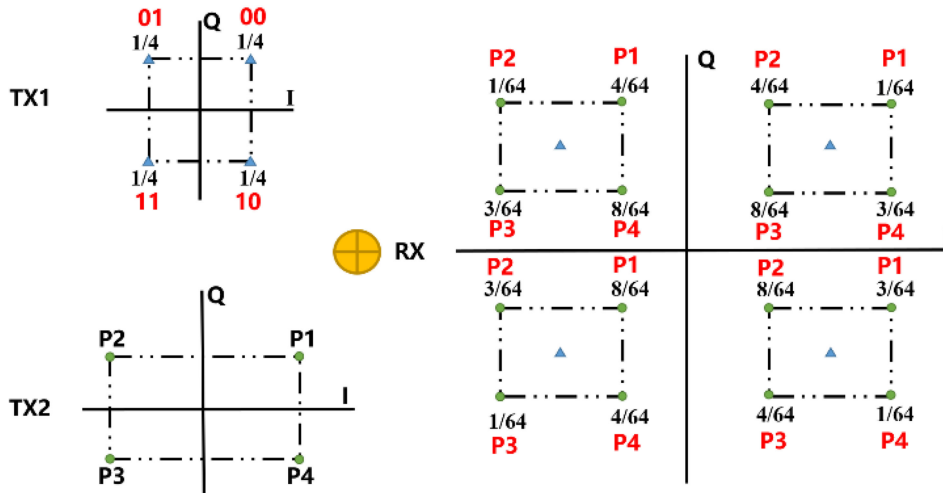
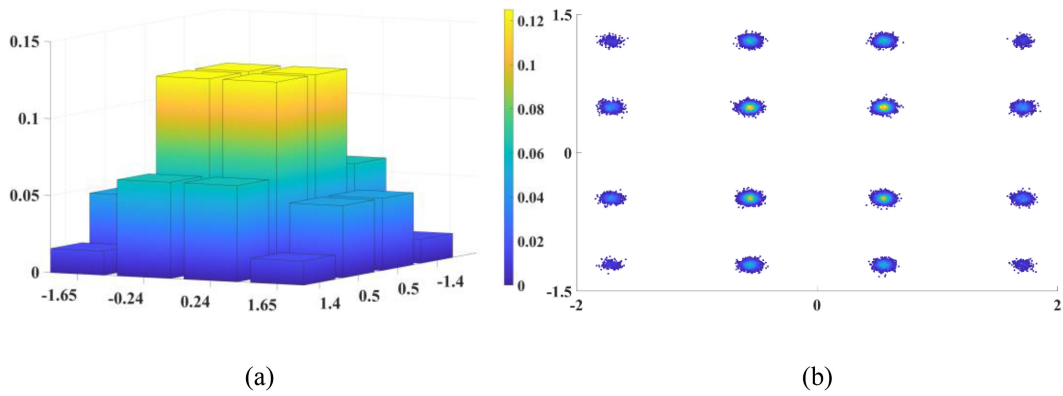Fig. 3. The diagram of constellation superposition.

(a)   (b)

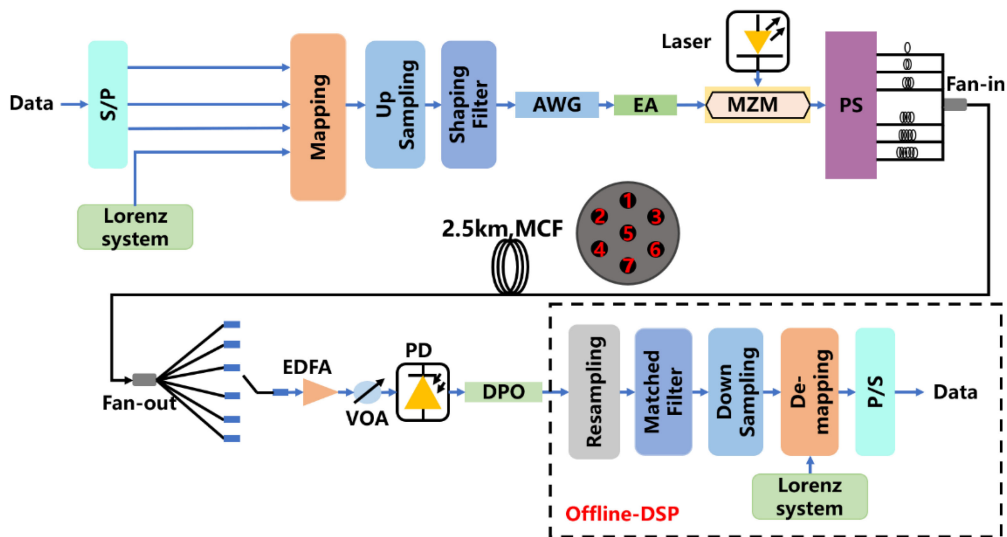Fig. 4. (a) Probability distribution. (b) Constellation diagram of the LS-PS-16CAP.

Fig. 5. Experimental setup (AWG: Arbitrary waveform generator; EA: Electrical amplifier; MZM: Mach-Zehnder modulator; PS: Power splitter; MCF: Multicore fiber; EDFA: Erbium-doped fiber amplifier; PD: Photodiode; DPO: Digital phosphor oscilloscope).

TABLE II
MAPPING RULES

(b4,b3,b2,b1)	First quadrant/00	Second quadrant/01	Third quadrant/11	Fourth quadrant/10
0000	[-3, -1]	[3, -1]	[3, 1]	[-3, 1]
0001	[3, -1]	[-3, -1]	[-3, 1]	[3, 1]
0010	[-3, -1]	[3, -1]	[3, 1]	[-3, 1]
0011	[3, -1]	[-3, -1]	[-3, 1]	[3, 1]
0100	[-3, 1]	[3, 1]	[3, -1]	[-3, -1]
0101	[-3, -1]	[3, -1]	[3, 1]	[-3, 1]
0110	[-3, 1]	[3, 1]	[3, -1]	[-3, -1]
0111	[-3, -1]	[3, -1]	[3, 1]	[-3, 1]
1000	[-3, 1]	[3, 1]	[3, -1]	[-3, -1]
1001	[-3, -1]	[3, 1]	[3, 1]	[-3, 1]
1010	[3, -1]	[-3, -1]	[-3, 1]	[3, 1]
1011	[-3, -1]	[3, -1]	[3, 1]	[-3, 1]
1100	[-3, -1]	[3, -1]	[3, 1]	[-3, 1]
1101	[-3, 1]	[3, 1]	[3, -1]	[-3, -1]
1110	[-3, -1]	[3, -1]	[3, 1]	[-3, 1]
1111	[3, 1]	[-3, 1]	[-3, -1]	[3, -1]

Fig. 7. BER curves of proposed PS-CAP16 in MCF fiber after 2.5 km transmission.
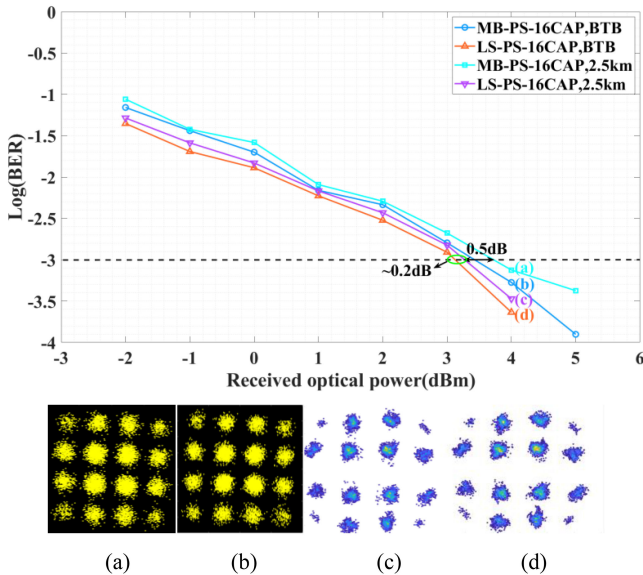

Fig. 6. BER curves of MB-PS-16CAP and LS-PS-16CAP in core3 for back-to-back (BTB) configuration and 2.5 km MCF transmission.

To be more specific, the Lorenz model is used as the chaotic model in the bits mapping stage to generate three chaotic sequences that can be expressed as follows:

$$\begin{cases} \dot{x} = a(y - x) \\ \dot{y} = bx - y - xz. \\ \dot{z} = -cz + xy \end{cases} \qquad (1)$$

Where a and b are the system parameters, which are 10 and 28 respectively, and c is the state feedback variable, which is 8/3. The parameters x, y, and z are system state variables, and the initial values of (x_0, y_0, z_0) are set as $(-1.6, -0.5, 21)$. To avoid the decrease of system sensitivity, the (1) is solved via the Runge-Kutta method with a time step of $h = 0.001$ [25]. The projections of the chaotic attractor for the Lorenz system in the three-dimensional space are illustrated in Fig. 2.
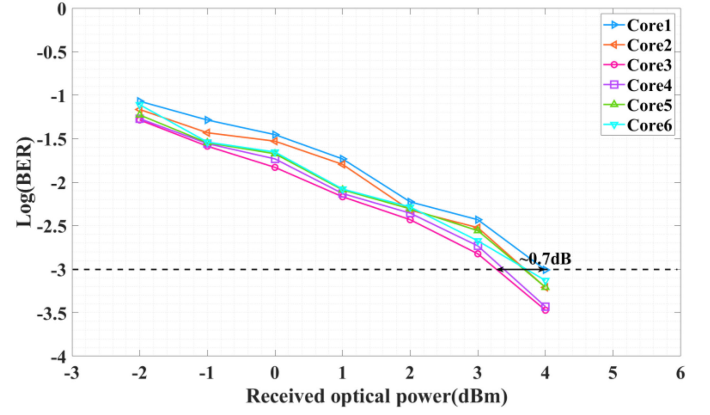
Three chaotic sequences x, y, and z are utilized to generate the bit sequences for rectangle-shaped 4QAM mapping, as shown in follows:

$$\begin{cases} b1 = floor(mod(x * 1e14, 2)) \\ b2 = floor(mod(y * 1e14, 2)) \\ b3 = floor(mod(z * 1e14, 2)) \end{cases} \qquad (2)$$

Where the function $floor\,(\varphi)$ rounds the elements of φ to the nearest integers, and $mod\,(j, k)$ returns the remainder of j divided by k. Then, the generated scrambled sequences {b1, b2, b3} and the information bit sequence b4 are mapped to a rectangular 4QAM.

The construction process of the LS-PS-16CAP constellation is shown in Fig. 3. The square-shaped 4QAM in TX1 are 1/4 uniform distribution. The rectangle-shaped 4QAM in TX2 is unequal distribution, as shown in Table I. The mathematical formula of the LS-PS-16QAM can be expressed as:

$$X_{PS-16QAM} = \alpha * X1_{4QAM} + X2_{4QAM}. \qquad (3)$$

Where $X1_{4QAM}$ are the square-shaped constellation points in TX1, $X2_{4QAM}$ are the rectangle-shaped 4QAM constellation points in TX2. The constellation points are linearly superposed to each other at the receiver, defined by $X_{PS-16QAM}$. Power coefficient α is expressed as the power ratios of the square-shaped 4QAM and the rectangle-shaped 4QAM signals, where the powers of both the 4QAM constellations are normalized.

The probability distribution of constellation points in TX2 is related to the quadrant of TX1 constellation points. The relationships of probability distribution for rectangle-shaped 4QAM constellation points are shown in Table I. For example, the probability distribution of TX1 constellation points in the first quadrant are P1 = 1/16; P2 = 4/16; P3 = 8/16; P4 = 3/16. The constellation points of TX1 in the first quadrant are then superimposed with those of TX2 to produce four different constellation points in the first quadrant of the LS-PS-16CAP signal. The probability of the constellation points in RX is shown in Fig. 3. Map rectangle-shaped constellation points using b4, b3, b2, and b1. The mapping rules of rectangle-shaped 4QAM are provided in Table II. b6 and b5 are used to map square-shaped constellation points corresponding to the LS-PS-16CAP quadrants.

TABLE III
PARAMETERS AND VALUES OF SEVEN-CORE FIBERS AND FIFO MODULES

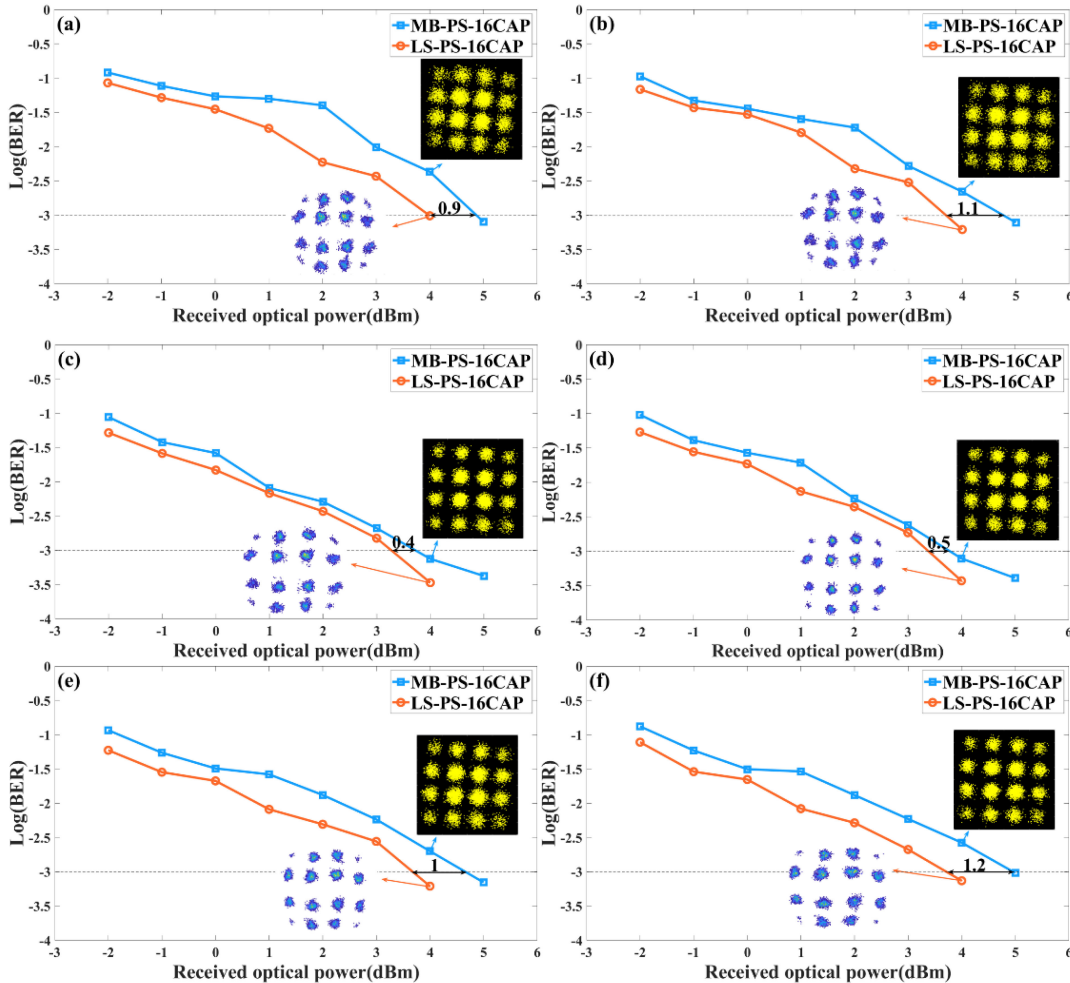|	Parameters	Values
Seven-core fibers	Crosstalk between cores	-50dB/100km
	Attenuation	0.25dB/km
	Mode field diameter	9.5μm
	Core layer diameter	7.9μm
	Core spacing	41.5±1.5μm
FIFO modules	Maximum insertion loss	1.5dB
	Crosstalk index (adjacent fiber)	-55dB

Fig. 8.   BER curves and corresponding constellations of MB-PS-16CAP and LS-PS-16CAP in core1 to core6.
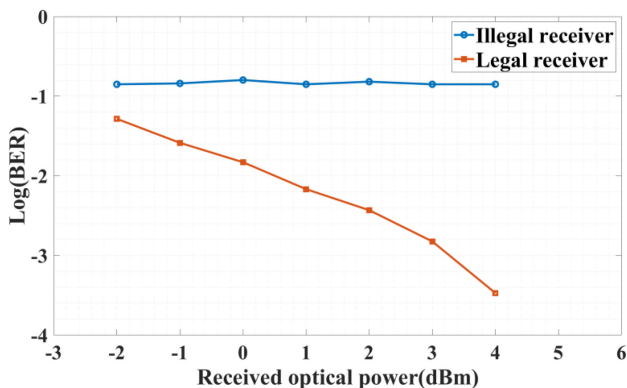

Fig. 9.   Bit error rate curve of legal receiver and illegal receiver.

III. EXPERIMENTAL SETUP AND RESULTS

Fig. 5 illustrates the experimental setup for the LS-PS-16CAP in the MCF transmission system. At the transmitter, the encrypted transmission signal is obtained by Lorenz chaos model and superposition, followed by an up-sampling and shaping filter. And then fed to the arbitrary waveform generator operated at 64GSa/s. After the amplification by an electrical amplifier, the electrical PS-16CAP signal and the laser's output 1550 nm light are passed through MZM for intensity modulation to generate a modulated optical signal. The optical signal is sent into MCF after passing through the 1:6 power splitter (PS) and fan-in device. After 2.5 km transmission in the MCF, the signal is demodulated by the fan-out device. EDFA is used to amplify the signal and a variable optical attenuator (VOA) is applied to adjust

the power. Finally, a photodetector detects the optical signal and converts it to electronic signal. The signal is collected using a Tektronix DPO72004C digital phosphor oscilloscope with a 100 GSa/s sampling rate and a 20 GHz bandwidth. Then perform offline digital signal processing (DSP) to recover the original signal and calculate bit error rate (BER). The detailed parameter settings of each device in the system are shown in Table III.

Fig. 6 displays the BER curves of MB-PS-16CAP and LS-PS-16CAP for BTB configuration and 2.5 km MCF transmission. It can be seen that there is 0.2 dB SNR penalty at the BER threshold of 1×10^{-3} after MCF transmission for LS-PS-16CAP. The received optical power at BER of 1×10^{-3} for MB-PS-16CAP and LS-PS-16CAP is 3.8 dBm and 3.3 dBm, respectively, with an improved gain is 0.5 dB. Fig. 6(a)–(d) shows a comparison of constellation diagrams of MB-PS-16CAP and LS-PS-16CAP signals after 2.5 km and BTB transmission at 4 dBm, respectively.

Fig. 7 shows the BER curves of LS-PS-16CAP in 6-core fiber after 2.5 km transmission. When BER is 1×10^{-3}, the received optical power of core1 to core6 is 4 dBm, 3.7 dBm, 3.3 dBm, 3.4 dBm, 3.7 dBm, and 3.72 dBm, respectively. The maximum power difference between core1 and core3 is about 0.7 dB. The performance of the fiber core varies as it relates to the fiber core parameters influenced by the manufacturing process.

The BER curves of MB-PS-16CAP and LS-PS-16CAP in core1 to core6 are shown in Fig. 8(a)–(f), respectively. At the same entropy of 3.7 bits/symbol, the proposed scheme outperforms the MB distribution, demonstrating the superiority of the proposed probabilistic shaping scheme. The gain obtained in each core is 0.9 dBm, 1.1 dBm, 0.4 dBm, 0.5 dBm, 1 dBm, and 1.2 dBm at BER of 1×10^{-3}, compared with MB-PS-16CAP. The difference in performance between the cores may be due to the different losses in the fan-in and fan-out devices. In addition, the environment can also affect the received optical power. The inset in Fig. 8 shows the constellation diagram for 4 dBm at the receiver through two given constellation schemes for each core.

To verify the security of the proposed LS-PS-16CAP, Fig. 9 depicts the BER curves of the legal receiver and the illegal receiver after 2.5 km MCF transmission in core3. The legal receiver exhibits better BER performance compared to the illegal receiver. For the illegal receiver, the BER is still stably maintained by about 0.15 even with the received optical power increasing, which makes the cracking on the transmitted signal impossible. We consider only three initial values and time step h. The key space of the proposed scheme can be calculated as $10^{14} \times 10^{14} \times 10^{15} \times 10^3 = 10^{46}$. The Fig. 9 shows that the proposed scheme can resist illegal attacks.

IV. CONCLUSION

In this paper, a novel LS-PS-16CAP constellation scheme is proposed to achieve constellation probability shaping by using the Lorenz model and the superposition principle. A 186.9 (31.6×6) Gb/s LS-PS-16CAP signal transmission over 2.5 km MCF is experimentally demonstrated. The experimental results show that the performance of the proposed LS-PS-16CAP outperforms the traditional MB-PS-16CAP counterpart by 0.7 dB gain at a BER of 1×10^{-3}. It can be seen that the novel constellation probabilistic shaping scheme has security and confidentiality and can effectively improve the BER

performance in the multi-core transmission, which proves it's an efficient solution for the future optical transmission system.

REFERENCES

[1] X. Zhang et al., "On throughput optimization in software-defined multi-dimensional space division multiplexing optical networks," J. Lightw. Technol., vol. 39, no. 9, pp. 2635–2651, May 2021.

[2] D. D. Falconer, "Carrierless AM/PM," Bell Labs., New York, NY, USA: Tech. Memo, 1975.

[3] X. Tang, I. L. J. Thng, and X. Li, "A new digital approach to design 3D CAP waveforms," IEEE Trans. Commun., vol. 51, no. 1, pp. 12–16, Jan. 2003.

[4] G. Cossu, A. M. Khalid, P. Choudhury, R. Corsini, and E. Ciaramella, "3.4 Gbit/s visible optical wireless transmission based on RGB LED," Opt. Exp., vol. 20, no. 26, pp. B501–B506, Dec. 2012.

[5] F. Hu, P. Zou, G. Li, W. Yu, and N. Chi, "Enhanced performance of CAP-modulated visible light communication system utilizing geometric shaping and rotation coding," IEEE Photon. J., vol. 11, no. 5, Oct. 2019, Art no. 7905412.

[6] F. Steiner and G. Böcherer, "Comparison of geometric and probabilistic shaping with application to ATSC 3.0," in Proc. 11th Int. ITG Conf. Syst. Commun. Coding, Feb. 2017, pp. 1–6.

[7] G. Bocherer, F. Steiner, and P. Schulte, "Bandwidth efficient and rate-matched low-density parity-check coded modulation," IEEE Trans. Commun., vol. 63, no. 12, pp. 4651–4665, Dec. 2015.

[8] A. Fallahpour et al., "16-QAM probabilistic constellation shaping by adaptively modifying the distribution of transmitted symbols based on errors at the receiver," Opt. Lett., vol. 45, no. 18, pp. 5283–5286, Sep. 2020.

[9] Y. Yao, K. Xiao, B. Xia, and Q. Gu, "Design and analysis of rotated-QAM based probabilistic shaping scheme for Rayleigh fading channels," IEEE Trans. Wireless Commun., vol. 19, no. 5, pp. 3047–3063, May 2020.

[10] X. Guo and N. Chi, "Superposed 32QAM constellation design for 2×2 spatial multiplexing MIMO VLC systems," J. Lightw. Technol., vol. 38, no. 7, pp. 1702–1711, Apr. 2020.

[11] J. Ren et al., "Three-dimensional probabilistically shaped CAP modulation based on constellation design using regular tetrahedron cells," J. Lightw. Technol., vol. 38, no. 7, pp. 1728–1734, Apr. 2020.

[12] A. Fallahpour et al., "16-QAM probabilistic constellation shaping by learning the distribution of transmitted symbols from the training sequence," in Proc. Conf. Opt. Fiber Commun., 2020, Paper M1G.3.

[13] Z. Dong, Y. Chen, X. Zhao, L. Zhou, and F. Li, "DMT transmission in short-reach optical interconnection employing a novel bit-class probabilistic shaping scheme," J. Lightw. Technol., vol. 39, no. 1, pp. 98–104, Jan. 2021.

[14] C. F. Zhang, W. Zhang, C. Chen, X. J. He, and K. Qiu, "Physical-enhanced secure strategy for OFDMA-PON using chaos and deoxyribonucleic acid encoding," J. Lightw. Technol., vol. 36, no. 9, pp. 1706–1712, Jan. 2018.

[15] M. W. Cui et al., "Chaotic RNA and DNA for security OFDM-WDM-PON and dynamic key agreement," Opt. Exp., vol. 29, no. 16, pp. 25552–25569, Jul. 2021.

[16] T. W. Wu et al., "Compressive sensing chaotic encryption algorithms for OFDM-PON data transmission," Opt. Exp., vol. 29, no. 3, pp. 3669–3684, Jan. 2021.

[17] Z. Zhang, Y. F. Luo, C. F. Zhang, X. S. Liang, M. W. Cui, and K. Qiu, "Constellation shaping chaotic encryption scheme with controllable statistical distribution for OFDM-PON," J. Lightw. Technol., vol. 40, no. 1, pp. 14–23, Jan. 2022.

[18] R. Tang et al., "Security strategy of parallel bit interleaved FBMC/OQAM based on four-dimensional chaos," Opt. Exp., vol. 29, no. 15, pp. 24561–24575, Jul. 2021.

[19] J. Ren et al., "Chaotic constant composition distribution matching for physical layer security in a PS-OFDM-PON," Opt. Exp., vol. 28, no. 26, pp. 39266–39276, Dec. 2020.

[20] D. Kumar and R. Ranjan, "Design and cross talk optimization in single-mode high-core count multicore fiber under limited cladding diameter," Opt. Eng., vol. 58, no. 5, May 2019, Art. no. 056109.

[21] D. J. Richardson, J. M. Fini, and L. E. Nelson, "Space-division multiplexing in optical fibres," Nature Photon., vol. 7, no. 5, pp. 354–362, Apr. 2013.

[22] B. J. Puttnam, G. Rademacher, and R. S. Luís, "Space-division multiplexing for optical fiber communications," Optical, vol. 8, no. 9, pp. 1186–1203, Sep. 2021.

[23] G. Rademacher et al., "10.66 Peta-Bit/s transmission over a 38-core-three-mode fiber," in Proc. Conf. Opt. Fiber Commun., 2020, Paper Th3H.1.

[24] G. Rademacher et al., "Space-division multiplexed transmission in the S-band over 55 km few-mode fibers," Opt. Exp., vol. 28, no. 18, pp. 27037–27043, Aug. 2020.

[25] N. Razali, R. R. Ahmad, M. Darus, and A. S. Rambely, "Fifth-order mean Runge-Kutta methods applied to the Lorenz system," in Proc. 13th WSEAS Int. Conf. Appl. Math., Dec. 2008, pp. 333–338.